Eur. Phys. J. D **6**, 235–241 (1999)

THE EUROPEAN PHYSICAL JOURNAL D

EDP Sciences

Magnetic moments of Ni_N clusters ($N \leq 34$): relation to atomic structure

J.L. Rodríguez-López[1,a], F. Aguilera-Granja[1], A. Vega[2], and J.A. Alonso[2]

[1] Instituto de Física, Universidad Autónoma de San Luis Potosí, 78000 San Luis Potosí, Mexico
[2] Departamento de Física Teórica, Universidad de Valladolid, E-47011 Valladolid, Spain

Received: 24 June 1998 / Received in final form: 12 November 1998

Abstract. We have calculated the magnetic moment per atom of nickel clusters (Ni_N) as a function of cluster size in the range $N \leq 34$ for the geometries proposed in the literature, obtained from different semi-empirical potentials. The spin-polarized electronic structure has been calculated with a self-consistent tight-binding method considering the $3d$, $4s$ and $4p$ valence electrons. We discuss the influence of geometrical factors like bond distance and coordination number. Good overall agreement with experiment is obtained, but some discrepancies remain.

PACS. 36.40.Cg Electronic and magnetic properties of clusters – 75.30.Pd Surface magnetism – 75.50.-y Studies of specific magnetic materials

1 Introduction

Several experimental measurements [1,2] and theoretical calculations [3–8] of the magnetic properties of nickel clusters have been done in recent years motivated by their possible technological applications as well as for the interest in their fundamental properties. Those calculations attempt to explain the behavior of the magnetic moment (per atom) as a function of the cluster size [1,2] in ferromagnetic clusters. The experimental results reported by Apsel *et al.* [1] are the most precise measurements nowadays for the average magnetic moment $\bar{\mu}$ in Ni clusters. These Stern-Gerlach deflection experiments have been performed for size selected clusters between Ni_5 and about Ni_{700} and a non-monotonic behavior of $\bar{\mu}$ was observed, in particular for the region below Ni_{100}, in agreement with the previous measurements by Billas *et al.* [2]. An overall decrease of the average magnetization with increasing cluster size is accompanied by oscillations displaying a strong reduction of the magnetization for certain sizes (sharp minima occur at Ni_6 and Ni_{13}, and broad minima around Ni_{34} and Ni_{56}) and a strong increase for other sizes (sharp maxima at Ni_5, Ni_8 and Ni_{71} and broad maxima around Ni_{20} and Ni_{42}).

It is generally accepted that the main factors that influence the behavior of the magnetic moments of small clusters are: i) the low atomic coordination of the atoms on the surface of the cluster [3], ii) the deviation of the inter-atomic distances with respect to the bulk values, and iii) the de-localization of the *sp* electrons near the Fermi level [4], that produces an indirect control of the number of holes in the *d* bands, particularly for the late transition metals. The first two factors are purely geometrical effects and the last one is electronic although, of course, the geometrical factors have a manifestation on the electronic structure. Developing a model that accounts for all those ingredients is a stringent challenge and the task is even harder considering that the geometrical structure of small clusters is unknown and very difficult to determine since often the structures found are different depending on the theoretical method used.

Ideally one would like to perform an *ab initio* calculation in which the lowest energy atomic arrangement is determined together with the electronic structure and average magnetic moment, as done for instance by Reuse and Khanna [8]. This procedure is, in practice, restricted to clusters with a small number of atoms, $N \leq 10$. For larger clusters the usual approach has been to calculate the electronic structure by the tight-binding (TB) formalism for structures previously determined (a) by assuming that the cluster is a fragment of a crystalline lattice [3,7] or (b) by using different model inter-atomic many-body potentials [9,10]. Andriotis *et al.* [5] have determined, however, both atomic structures and magnetic moments from a TB-molecular dynamics method.

Experiments measuring the saturation coverage of Ni_N by weakly reactive molecules give also information about the structure of those clusters [11]. The analysis of those experiments appears to be consistent with a pattern of icosahedral growth, at least for sizes not far from the main shell closing numbers ($N = 13, 55, ...$) [10], but the situation is not clear for other sizes. The comparison of calculated and measured magnetic moments can provide an indirect test of cluster geometries. So far only a few

[a] e-mail: puma@dec1.ifisica.uaslp.mx

studies involving a range of cluster sizes large enough to make a comparison with experiment meaningful have been published [3,4,6,7]. Jensen *et al.* [3] and Guevara *et al.* [7] assumed the structure to be close to a crystalline fragment, which is rather restrictive. In a previous work [6] we have calculated the spin-polarized electronic structure by solving self-consistently a tight-binding Hamiltonian for the $3d$, $4s$ and $4p$ valence electrons of Ni_N clusters in a mean-field approximation. The structures were fully optimized for $N \leq 20$ using molecular dynamics and a semi-empirical many-body potential based on TB ideas [12]. The calculated geometries indicate an icosahedral type of growth, so for $N \geq 21$ the same potential was used for a steepest-descent relaxation method, starting with icosahedral structures. The conclusion of that study was that the observed main minima of $\bar{\mu}$, at $N = 13$, $N = 55$ and around $N = 34$, are reproduced by the calculations, but the maxima in between are not reproduced well. The source of the discrepancies may be twofold. On one hand the atomic structures far from the main minima of $\bar{\mu}$ may be different from the icosahedral-like motifs assumed. On the other hand, the parameterized TB method used to calculate the electronic structure may not be flexible enough to describe well the de-localized *sp* levels near the Fermi energy ε_F, which indirectly affect the occupation of the up and down spin d bands. As an attempt to shed some light into this problem, we now undertake the calculation of the magnetic moments of the Ni clusters for different geometries taken from several calculations recently published using, as in our previous work, a TB Hamiltonian with $3d$, $4s$ and $4p$ valence electrons. The geometries used in the present calculations are those determined by Nayak *et al.* [13] and Hu *et al.* [14]. By comparing the results of the electronic structure under the same calculational scheme and approximations for different sets of geometries proposed in the literature, we expect to disentangle the effects of incorrect geometries from those due to approximations involved in the calculation of the electronic structure. In Section 2, we present the theoretical model used in this work and section 3 explains the geometrical characteristics of the clusters. The results and their analysis are given in Section 4. We conclude with a brief summary in Section 5.

2 Model and approximations

The spin-polarized electronic structure has been determined for each geometrical arrangement of the Ni_N clusters by solving self-consistently a tight-binding Hamiltonian for the $3d$, $4s$ and $4p$ valence electrons in a mean-field approximation. The non-diagonal elements of the Hamiltonian are assumed spin-independent and are obtained using the Slater-Koster approximation taking the two-center hopping integrals from Papaconstantopoulos, who fitted them to reproduce the band structure of fcc bulk nickel [15]. Since the interatomic distances in the clusters [16] differ a little from the distances in the bulk, we have assumed the hopping integrals in the neighborhood of the ideal first- and second-nearest-neighbors values to follow the usual power law $(r_0/r_{ij})^{l+l'+1}$, where r_0 is the bulk first (second) nearest-neighbor distance and l, l' are the orbital angular momenta of the spin-orbitals involved in the hopping process [17]. This scaling law is only approximate, and an exponential decay has been sometimes used [18]. In fact the ratio of the first and second neighbor integrals fitted by Papaconstantopoulos does not obey the $(r_0/r_{ij})^{l+l'+1}$ law for some Slater-Koster integrals. Nevertheless, tests have been performed that indicate that reasonable changes in the scaling law or in the basic fitted parameters do not produce significant changes in the magnetic moments [19]. The diagonal terms of the Hamiltonian are spin-dependent via the electron-electron interaction, which appears as a correction shift of the orbital energy levels in a mean-field approximation

$$\varepsilon_{i\alpha\sigma} = \varepsilon^0_{i\alpha} + z_\sigma \sum_\beta \frac{J_{\alpha\beta}}{2} \mu_{i\beta} + \Omega_{i\alpha}\,, \tag{1}$$

where i indicates the atomic site, α and β stand for the type of orbital (s, p, d) and σ is the spin projection. $\varepsilon^0_{i\alpha}$ are the orbital energies taken from the fit of Papaconstantopoulos for paramagnetic bulk Ni, and consequently do not incorporate the magnetic contribution, although they implicitly contain the rest of the electron-electron interactions as well as the crystalline field of the bulk. The variations of the last two contributions when one considers the clusters, instead of the bulk, are accounted for by the potentials $\Omega_{i\alpha}$. The second term in equation (1) is the spin-dependent shift due to the spin-polarization $\mu_{i\beta} = n_{i\beta\uparrow} - n_{i\beta\downarrow}$ of the electrons at site i and orbital β, calculated from the occupation numbers $n_{i\beta\sigma}$. In this term, $J_{\alpha\beta}$ are the exchange interaction parameters and z_σ is the sign function ($z_\uparrow = 1$, $z_\downarrow = -1$). All the exchange parameters involving s and p electrons are neglected and J_{dd} is fitted in order to reproduce the bulk magnetic moment. Note that spin-polarization of the delocalized *sp* band will also occur as a consequence of the hibridization with the spin-polarized d-states. Finally, the site- and orbital-dependent potentials $\Omega_{i\alpha}$ (Ω_{id}, $\Omega_{is} = \Omega_{ip}$) are self-consistently determined in order to assure the *sp* and d electronic occupations at each site within the cluster, fixed in our model by a linear interpolation between the isolated atom (d^8, s^2, p^0) and the bulk ($d^{9.1}$, $sp^{0.9}$) configurations according to the local coordination number, and assuming local charge neutrality, that is a total of 10 *spd* electrons on each site. We have considered different potentials for the localized d-states (Ω_{id}) and for the delocalized *sp*-states ($\Omega_{is} = \Omega_{ip}$). The spin-dependent local electronic occupations are self-consistently obtained by integrating up to the Fermi level the local densities of states, which are calculated at each iteration by using the recursion method [20].

Table 1. Similarities and differences between the ground state structures of Ni_N clusters ($N \leq 15$) obtained with different potentials: Gupta (G), Finnis-Sinclair (FS), Lennard-Jones (LJ), Morse (M). When one structure is common to several potentials, this structure is outlined on the last column. The data for Ni_8 is given in Table 4.

N	(G) [9]	(FS) [13]	(LJ) [14]	(M) [14]	Common Structure
5	TB	TB	TB	TB	Trigonal Bipyramid (TB)
6	O	O	O	O	Octahedron (O)
7	PB	PB	PB	PB	Pentagonal Bipyramid (PB)
9	*a*	*b*	—	—	
10	PB+3	PB+3	—	—	Pentagonal Bipyramid+3 (PB+3)
11	PB+4	PB+4	PB+4	*c*	Pentagonal Bipyramid+4 (PB+4)
12	I−1	I−1	—	—	Icosahedron−1 (I−1)
13	I	I	I	I	Icosahedron (I)
14	I+1	I+1	—	—	Icosahedron+1 (I+1)
15	*d*	*e*	*d*	*e*	

[a]Octahedron+3. [b]Pentagonal bipyramid+2. [c]Hexahedron+6. [d]Icosahedron+2. [e]Hexagonal antiprysm.

Table 2. Number n_i of equivalent sites (and coordination Z_i), average coordination $\bar{Z}$ and average nearest-neighbor distance d_n as a function of cluster size N for the ground state geometries found by Nayak *et al.* [13].

Finnis & Sinclair			
N	$n_i\,(Z_i)$	$\bar{Z}$	d_n (Å)
2	2(1)	1.0	2.01
3	3(2)	2.0	2.11
4	4(3)	3.0	2.19
5	2(3), 3(4)	3.6	2.21
6	6(4)	4.0	2.24
7	5(4), 2(6)	4.57	2.25
8	4(4), 4(5)	4.5	2.25
9	4(4), 2(5), 2(6), 1(8)	5.11	2.26
10	3(4), 3(5), 3(6), 1(9)	5.4	2.26
11	2(4), 4(5), 4(6), 1(10)	5.64	2.25
12	5(5), 6(6), 1(11)	6.0	2.27
13	12(6), 1(12)	6.46	2.26
14	1(3), 9(6), 3(7), 1(12)	6.43	2.26
15	12(6), 2(7), 1(14)	6.67	2.24
16	1(4), 7(5), 7(6), 1(9)	5.63	2.27
17	2(4), 3(5), 11(6), 1(11)	5.88	2.27
18	2(4), 8(5), 8(7)	5.77	2.26
19	12(6), 5(8), 2(12)	7.16	2.27
20	2(5), 16(6), 2(11)	6.4	2.28
21	1(4), 4(5), 8(6), 4(7), 2(8), 1(10), 1(12)	6.57	2.26
22	5(5), 9(6), 4(7), 2(8), 1(9), 1(12)	6.54	2.28
23	2(5), 12(6), 6(7), 1(8), 2(12)	6.78	2.26

3 Geometrical structures selected for the Ni clusters

As mentioned in Section 1, calculations of the geometries of Ni clusters for most cluster sizes within wide size ranges have only been performed using semi-empirical inter-atomic potentials. Table 1 shows the similarities and differences between the structures obtained with those potentials for $N \leq 15$. When a structure is dominant, this is outlined on the last column of the table. Nayak *et al.* [13] performed molecular dynamics simulations with the Finnis-Sinclair (FS) potential [21], which is based on the TB method and contains many-body interactions; some geometrical characteristics of the cluster ground state up to $N = 23$ are presented in Table 2. Atoms in equivalent sites are grouped, and the Table gives the number of atoms in those groups (with their respective atomic coordination), the average coordination number in the cluster and the average nearest-neighbor distance. Plots of the cluster shapes are given in Nayak's paper [13]. The ground state structures of Hu *et al.* [14] correspond to the Lennard-Jones (LJ) and Morse (M) potentials, and were obtained by combining the Monte Carlo method and a fast relaxation algorithm of the molecular dynamics; plots of the cluster shapes are given in the original paper [14]. In this study we focus only on those clusters for which the LJ and the M potentials predict different structures. The geometrical characteristics of those clusters are presented

Table 3. Number n_i of equivalent sites (and coordination Z_i), average coordination $\bar{Z}$ and average nearest-neighbor distance d_n for the ground state geometries found by Hu *et al.* [14] using Lennard-Jones and Morse potentials.

Lennard-Jones			
N	$n_i\,(Z_i)$	$\bar{Z}$	d_n (Å)
8	1(3), 3(4), 2(5), 1(6), 1(7)	4.75	2.48
11	2(4), 4(5), 4(6), 1(10)	5.6	2.48
15	2(4), 8(6), 2(7), 2(8), 1(12)	6.5	2.48
17	2(4), 2(5), 6(6), 2(7), 2(8), 2(9), 1(12)	6.7	2.48
27	12(6), 8(8), 2(9), 1(10), 4(12)	7.8	2.50
29	12(6), 6(8), 6(9), 5(12)	8.1	2.51
32	2(5), 14(6), 2(7), 9(8), 5(12)	7.5	2.46
34	2(4), 2(5), 10(6), 6(7), 5(8), 4(9), 5(12)	7.5	2.46
Morse			
N	$n_i\,(Z_i)$	$\bar{Z}$	d_n (Å)
8	4(4), 4(6)	5	2.48
11	1(4), 6(5), 3(6), 1(10)	5.6	2.43
15	12(6), 2(7), 1(14)	6.7	2.41
17	3(4), 7(6), 3(7), 3(9), 1(12)	6.7	2.39
27	1(4), 10(6), 2(7), 5(8), 4(9), 1(10), 4(12)	7.8	2.36
29	12(6), 6(8), 6(9), 5(12)	8.1	2.36
32	12(6), 7(8), 6(9), 1(10), 6(12)	8.2	2.36
34	12(6), 5(8), 10(9), 7(12)	8.4	2.36

Table 4. Different structures proposed in the literature for Ni_8. Symbols as in Tables 2 and 3.

Structure (Potential)	$n_i\,(Z_i)$	$\bar{Z}$	d_n (Å)
Bicapped octahedron (Gupta) [9]	4(4), 4(5)	4.5	2.46
Saturated tetrahedron (Parks) [11]	4(3), 4(6)	4.5	2.43
Bicapped octahedron (Finnis and Sinclair) [13]	4(4), 4(5)	4.5	2.25
Capped pentagonal bipyramid (Lennard-Jones) [14]	1(3), 3(4), 2(5), 1(6), 1(7)	4.75	2.48
Deformed central tetrahedron (Morse) [14]	4(4), 4(6)	5.0	2.48

in Tables 3. For Ni_8 we have also considered a structure proposed by Parks *et al.* [11], induced from the analysis of their adsorption experiments. Table 4 presents a summary of the characteristics for the different structures considered for Ni_8. As can be seen, for some clusters several different structures have been proposed in the literature, as a consequence of the different type of potentials used.

4 Results and discussion

Prior to presenting the results of the electronic structure calculations, we comment on the geometrical characteristics of the clusters by comparing these with our previous calculations [6] based on the many-atom TB model potential developed by Gupta [12]. In Figure 1, we present the average nearest-neighbor distance as a function of the cluster size. The interatomic distances obtained by Nayak *et al.* are 0.2-0.3 Å smaller than the ones obtained with the Gupta potential. Both show a rather monotonic increase with the cluster size, fast up to about Ni_8 and then slow, but only the Gupta potential achieves the convergence to the bulk value of $d_n(\text{bulk}) = 2.49$ Å. In the same figure, we present Hu's results for M and LJ potentials. Interatomic distances in the LJ clusters are close to those from the Gupta potential and the Morse potential produces distances in between those of the LJ and Finnis-Sinclair potentials. For the Morse potential, the average nearest-neighbor distance has a rather unphysical behavior.

The average atomic coordination $\bar{Z}$ is presented in Figure 2. $\bar{Z}$ is insensitive to the type of inter-atomic potential for cluster sizes smaller than $N = 15$, except for $N = 8$, where some discrepancies exist. For larger clusters the coordination obtained by Nayak [13] using the FS potential is lower than the coordination obtained from the Gupta potential except for Ni_{19}. The LJ clusters have practically the same average coordination numbers as the clusters with Gupta potential and the same can be said of the Morse clusters with the exception of Ni_{32} and Ni_{34}, that present larger coordination. In Figures 1 and 2 we have also included the structure suggested by Riley *et al.* [11] for Ni_8.

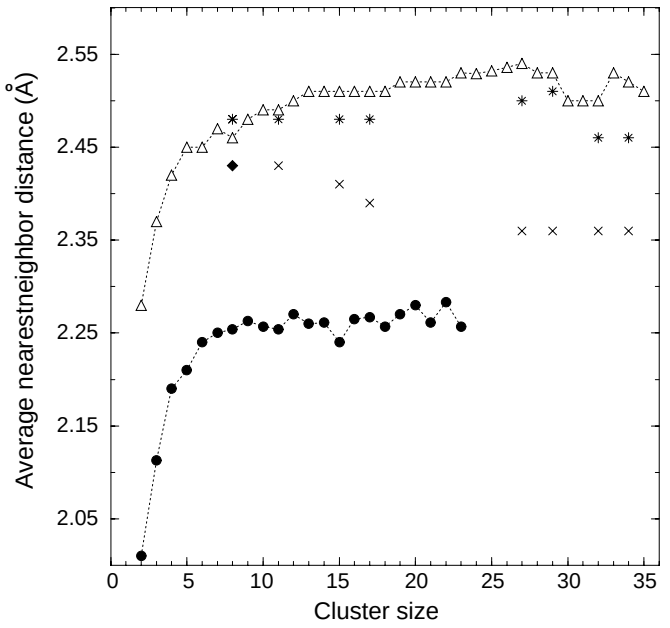

Fig. 1. Average nearest-neighbor distance d_n as a function of cluster size N for Ni_N clusters, obtained from: (●) Finnis-Sinclair potential [13], (∗) Lennard-Jones potential [14], (×) Morse potential [14] and (△) Gupta potential [6]. The additional result for Ni_8 (♦) corresponds to a structure proposed by Riley *et al.* [11].

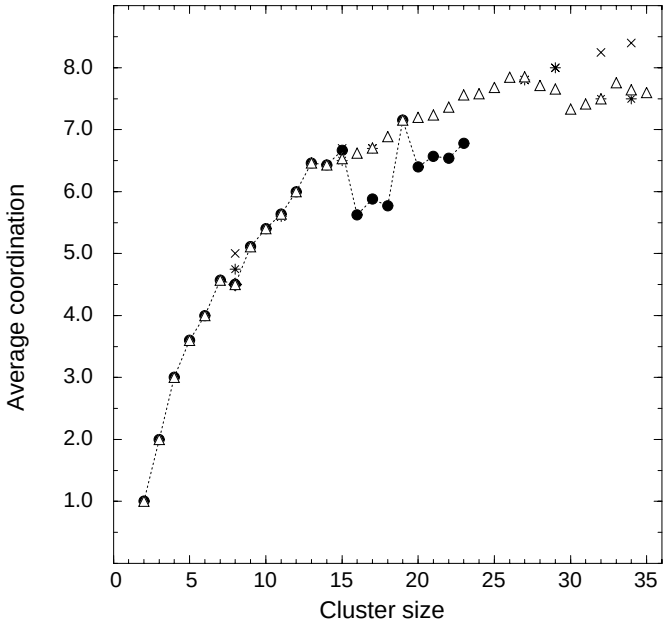

Fig. 2. Average atomic coordination as a function of cluster size N obtained from the Finnis-Sinclair, Lennard-Jones, Morse and Gupta potentials. Symbols as in Figure 1.

In Figures 3 and 4 we show the calculated magnetic moments together with the experimental results of Apsel *et al.* [1]. To clarify the comparison we plot first in Figure 3 the calculated magnetic moments for the structures obtained with the FS [13], LJ [14] and Morse potentials [14], compared with the experimental magnetic moments [1]. Then, in Figure 4 the same three sets of new theoretical results are compared to the previous results of Aguilera-Granja *et al.* [6] (Gupta potential and icosahedral growth) and to those of Andriotis *et al.* [5] obtained from tight-binding molecular dynamics. The common behavior to all the calculations is a decrease of the magnetic moment as the cluster size increases, the differences arising in the details of the oscillations superimposed to the overall decrease. The overall decrease of $\bar{\mu}$ with N can be seen as a consequence of the growing average coordination which occurs as the fraction of surface atoms in the cluster decreases. Concerning this overall behavior of $\bar{\mu}$, all the theoretical calculations predict a steeper decrease compared to experiment; in the region around Ni_{34}, the calculated moments are closer to the magnetic moment of bulk nickel. The minima of $\bar{\mu}$ in Ni_6 and Ni_{13} reported experimentally are reproduced by the structures found by Nayak [13], although the minimum at Ni_{13} is very shallow. Additional calculated minima occur at $N = 15$ and $N = 18$, while shallow minima are measured at $N = 16$ and 19. Local maxima of $\bar{\mu}$ are predicted at Ni_7, Ni_{14}, Ni_{16}, Ni_{20} and Ni_{22}, in reasonable agreement with the measured ones at Ni_8, Ni_{15}, Ni_{17}, Ni_{20} and Ni_{22}. The drop between Ni_{20} and Ni_{21} agrees with experiment, although the calculation exaggerates that drop. In summary, the magnitude of the oscillations of $\bar{\mu}$ obtained for the FS geometries is too large compared to experiment, except for the minimum at Ni_{13} in which case the opposite occurs: the theoretical local minimum is too shallow. The structures determined with the Gupta potential [6] produce a more accurate behavior of $\bar{\mu}$ for small clusters (the correct minimum at Ni_6 and maximum at Ni_8, and a deep minimum at Ni_{13}) but $\bar{\mu}$ decreases monotonically between Ni_{14} and Ni_{23}. Notice that in the size range $N \leq 20$ the structures we are comparing are obtained, for both potentials (Finnis-Sinclair and Gupta), from fully unconstrained MD, and that these structures are rather similar, as revealed by the identical average coordination (Fig. 2), except in a few cases with $N \geq 15$. These structural differences for $N \geq 15$ account for the differences in the behavior of $\bar{\mu}$ in that size region. Also, another important difference is that the FS structures lead to lower values of $\bar{\mu}$ (except in a few exceptional cases) and this is certainly ascribed to the shorter inter-atomic separations of Figure 1. In conclusion, compared to experiment, the overall predictions of the FS and Gupta potentials are rather similar although there are some differences of detail, especially for $N \geq 15$. Both potentials fail to reproduce the approximate constancy of $\bar{\mu}$ between Ni_{14} and about Ni_{22} observed by Apsel *et al.* [1], so a possible misrepresentation of the correct cluster geometry does not appear to be the main source of discrepancies with experiment. In Figure 4 we observe that the LJ potential leads to structures that have magnetic moments similar to those from the Gupta potential. This is understandable in view of the similar average nearest-neighbor distances and coordination for the two potentials. The magnetic moments corresponding to the Morse structures are rather similar to those from

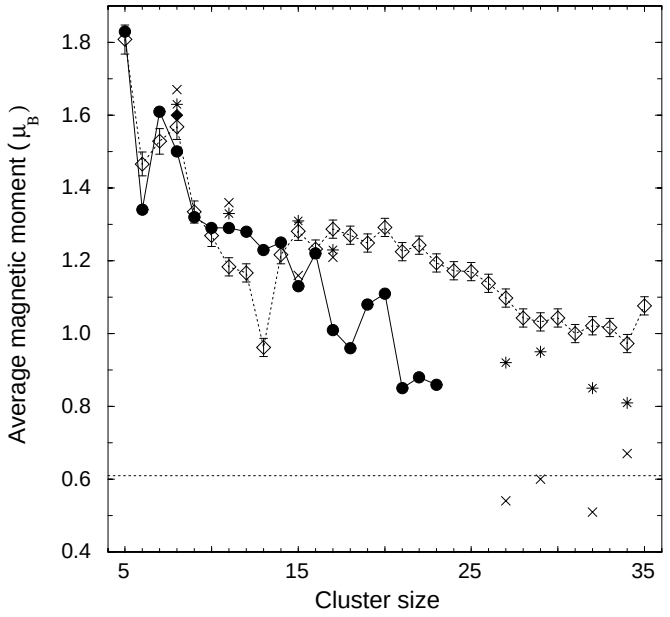

Fig. 3. Average magnetic moments for the new geometries considered in this work corresponding to the Finnis-Sinclair, Lennard-Jones and Morse potentials (symbols as in Fig. 1) compared to experimental results (◇) with error bars as given by Apsel *et al.* [1]. Horizontal dotted line indicates the measured bulk value.

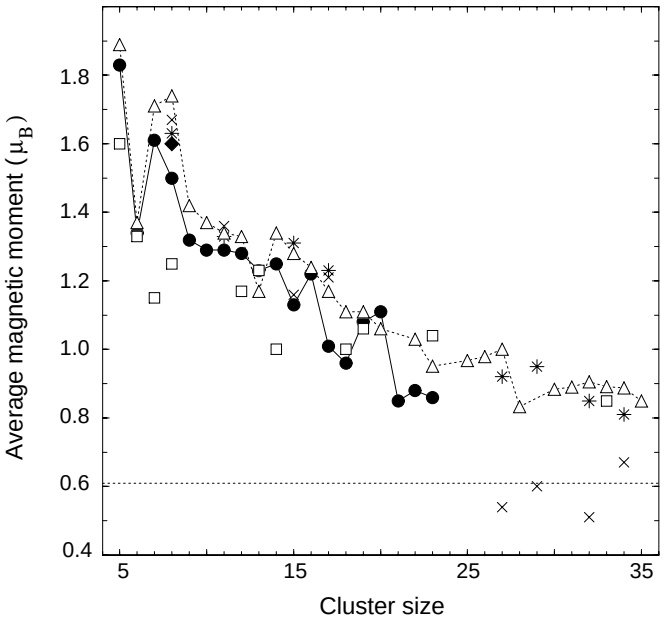

Fig. 4. Calculated average magnetic moment per atom as a function of cluster size for Finnis-Sinclair, Lennard-Jones, Morse and Gupta geometries (symbols as in Fig. 1). Also results from tight-binding molecular dynamics (▫) after Andriotis [5].

other potentials for small N, but become too low for large N, becoming even smaller than the bulk moment. This is also a consequence of the small inter-atomic distances displayed in Figure 1. Figures 3 and 4 also include the result for the structure suggested by Riley *et al.* [11] for Ni_8 and the agreement with the experimental magnetic moment is fairly good. Furthermore, in Figure 4, we also include the results of Andriotis *et al.*, also based on a TB method but with geometrical structures obtained by TB-molecular dynamics [5]. The magnitude of $\bar{\mu}$ is similar to the other predictions and the detailed behavior is not better. One can notice the failure to reproduce the observed minima at $N = 6$ and $N = 13$. The limited number of cluster sizes makes a more detailed comparison difficult.

In conclusion, the differences in average magnetic moments produced by the structures predicted by the different interatomic potentials analyzed here are driven mainly by differences in interatomic distances which affect, first of all, the hopping integrals and then the electronic structure through self-consistency. Lower interatomic distances result in smaller magnetic moments. This is, nevertheless, not the only source of discrepancies between the various calculations. Intrinsic structural differences account also for differences of $\bar{\mu}$. The average coordination reflects, to some extent, structural differences, although it is not a very precise indicator. For instance, the low average coordination in the FS structures for Ni_{16}-Ni_{18} and Ni_{20}-Ni_{23} only becomes reflected in high magnetic moments for Ni_{16} and Ni_{20}, but the other clusters have, instead, low magnetic moments. In Figure 5 we present the *sp* contribution to the magnetic moment as a function of the cluster size.

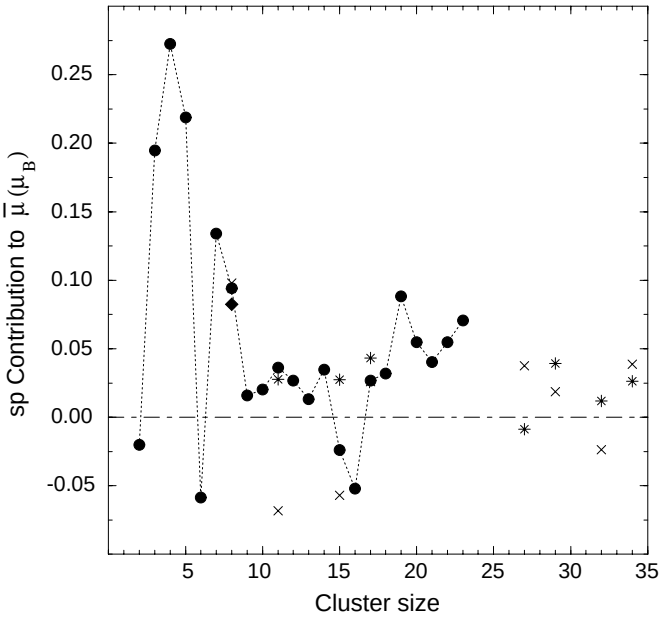

Fig. 5. Contribution of the *sp* magnetic moment as a function of the cluster size for Finnis-Sinclair, Lennard-Jones and Morse geometries. Symbols as in previous figures.

These results reinforce the view that the *sp* contribution is only important for small clusters and that it controls the oscillations of $\bar{\mu}$ for small N as we have reported previously [6].

5 Summary

We have compared the results of calculations of the magnetic moments of nickel clusters using a tight-binding formalism and several different proposals for the geometrical structures given in the literature, obtained from different semi-empirical interatomic potentials and in one case from TB-molecular dynamics [5]. The results for the different sets of geometrical structures are roughly consistent with each other. Those show the overall decrease of $\bar{\mu}$ with cluster size, and predict the oscillations of $\bar{\mu}$ for small N reasonably well. All the calculations, however, give a faster decrease of $\bar{\mu}$ with N and predict a faster approach to the bulk value. In particular, the approximate constancy of $\bar{\mu}$ in the range between Ni_{14} and Ni_{20}, which has been suggested [6] that could be related to delocalization of the *sp* electrons near the Fermi level [4], remains largely unexplained and perhaps requires a theory beyond the TB formalism.

We are greatful to Prof. P. Jena, Dr. S.K. Nayak and Dr. W.J. Hu for providing us with atomic coordinates and detailed structures of clusters in references [13] and [14]. This work has been supported by DGES (Grant PB95-0720-C02-01) and by Junta de Castilla y León (Grant VA 72/96). Two of us (JLRL and FAG) also acknowledge support from CONACyT (Grant 625851-E), México.

References

1. S.E. Apsel, J.W. Emmert, J. Deng, L.A. Bloomfield, Phys. Rev. Lett. **76**, 1441 (1996).
2. I.M.L. Billas, A. Chatelain, W.A. de Heer, Science **265**, 1682 (1994); J. Magn. Magn. Mater. **168**, 64 (1997).
3. P.J. Jensen, K.H. Benneman, Z. Phys. D **35**, 273 (1995).
4. N. Fujima, T. Yamaguchi, Phys. Rev. B **54**, 26 (1996).
5. A.N. Andriotis, N.N. Lathiotakis, M. Menon, Europhys. Lett. **36**, 37 (1996); N. Lathiotakis, A.N. Andriotis, M. Menon, J. Connolly, J. Chem. Phys. **104**, 992 (1996).
6. S. Bouarab, A. Vega, M.J. López, M.P. Iniguez, J.A. Alonso, Phys. Rev. B **55**, 13279 (1997); F. Aguilera-Granja, S. Bouarab, M.J. López, A. Vega, J.M. Montejano-Carrizales, M.P. Iniguez, J.A. Alonso, Phys. Rev. B **57**, 12469 (1998).
7. J. Guevara, F. Parisi, A.M. Llois, M. Weissman, Phys. Rev. B **55**, 13283 (1997).
8. F.A. Reuse, S.N. Khanna, Chem. Phys. Lett. **234**, 77 (1995); F.A. Reuse, S.N. Khanna, S. Bernel, Phys. Rev. B **52**, 11650 (1995).
9. M.J. López, J. Jellinek, Phys. Rev. A **50**, 1445 (1994).
10. J.M. Montejano-Carrizales, M.P. Iñiguez, J.A. Alonso, M.J. López, Phys. Rev. B **54**, 5961 (1996).
11. E.K. Parks, B.J. Winters, T.D. Klots, S.J. Riley, J. Chem. Phys. **94**, 1882 (1991); E.K. Parks, L. Zhu, J. Ho, S.J. Riley, J. Chem. Phys. **100**, 7206 (1994); E.K. Parks, S.J. Riley, Z. Phys. D **33**, 59 (1995); E.K. Parks, G.C. Nieman, K.P. Kerns, S.J. Riley, J. Chem. Phys. **107**, 1861 (1997).
12. R.P. Gupta, Phys. Rev. B **23**, 6265 (1981).
13. S.K. Nayak, S.N. Khanna, B.K. Rao, P. Jena, J. Phys. Chem. A **101**, 1072 (1997).
14. W. Hu, L.M. Mei, H. Li, Solid State Commun. **100**, 129 (1996).
15. D.A. Papaconstantopoulos, *Handbook of the Band Structure of Elemental Solids* (Plenum, New York, 1996).
16. Atomic coordinates have been provided by the authors of references [13] and [14].
17. V. Heine, Phys. Rev. **153**, 673 (1967).
18. L. Goodwin, A.J. Skinner, D.G. Pettifor, Europhys. Lett. **9**, 701 (1989).
19. A. Vega, A. Mokrani, unpublished work.
20. R. Haydock, *Solid State Physics*, Vol. 35, edited by E. Ehrenreich, F. Seitz, D. Turnbull (Academic Press, London, 1980), p. 215.
21. M.W. Finnis, J.E. Sinclair, Philos. Mag. **50**, 45 (1984); A. Sutton, J. Chen, Philos. Mag. Lett. **61**, 139 (1990).